A new proposal to Jefferson Lab PAC31

Measurements of Double-Spin Asymmetries on a Transversely Polarized Proton Target in Semi-Inclusive DIS Reaction

R. Gilman, C. Glashausser, X. Jiang (Spokesperson)[a], G. Kumbartzki, E. Kuchina and R. Ransome
Rutgers University, Piscataway, New Jersey.

J.-P. Chen, M. Jones
Jefferson Lab, Newport News, Virginia.

A. Asaturyan, A. Mkrtchyan, H. Mkrtchyan and V. Tadevosyan
Yerevan Physics Institute, Yerevan, Armenia.

Abstract: We propose to measure the beam-target double-spin asymmetry ($\mathcal{A}_{LT}$) on a transversely polarized proton target in semi-inclusive deep-inelastic $p(e,e'\pi^+)$ reaction. In the leading order QCD parton model the double spin asymmetry $\mathcal{A}_{LT}$ arises due to the longitudinal polarization of quarks in the transversely polarized nucleon. The asymmetry $\mathcal{A}_{LT}$ is non-vanishing only if quarks have non-zero transverse momentum, thus non-zero angular momentum. Such a non-zero $\mathcal{A}_{LT}$ asymmetry in semi-inclusive DIS reactions has never been established experimentally. Several model calculations predict a few percent $\mathcal{A}_{LT}$ asymmetry for this experiment. In particular, if one ignores the gauge links, the corresponding transverse momentum (k_T) dependent quark distribution function g_{1T}^q can be related to the twist-three distribution function $g_2(x)$ through the much-debated Lorentz invariance relation. Under such an assumption, one also expects a sizable $\mathcal{A}_{LT}$ asymmetry. The goal of this experiment is to make the first definitive measurement of $\mathcal{A}_{LT}$ and the quark transverse momentum dependent distribution g_{1T} and to clearly establish if it is non-zero. The technical details of this experiment is mostly identical to that of the approved "semi-SANE" (E04-113) and "SANE" (E03-109) experiments. The large acceptance *BETA* detector, in the identical setting as in the SANE experiment, will be used to detect the scattered electrons at 40°. The HMS spectrometer will be used to detect π^+ at 2.3 GeV/c and 14° in coincidence ($z_\pi \approx 0.5$). The standard Hall C polarized NH_3 target will be used in its transverse setting identical to that of the SANE experiment. A total of 25 days of 6 GeV beam time is needed for this experiment, of which 10 days can be a shared time with the SANE experiment. **Therefore, we request approval of 15 days assuming the SANE experiment is re-approved.**

[a]Contact person, email: jiang@jlab.org

Contents

1 Introduction

In leading order QCD, when integrating over quark intrinsic transverse momentum, three parton distribution functions describe the momentum and spin of the quarks inside the nucleon. These are the quark density distribution $f_1^q(x, Q^2)$, the quark helicity distribution $g_1^q(x, Q^2)$, and the quark transversity distribution $h_1^q(x, Q^2)$ which describes quark transverse spin distribution in a transversely polarized nucleon. Over the past 35 years, many deep-inelastic scattering (DIS) experiments have been devoted to the detailed studies of quark momentum and helicity distributions. In the last few years, the HERMES experiment [1] at DESY and the COMPASS experiment [2] at CERN have reported results from semi-inclusive deep-inelastic scattering (SIDIS) data collected with transversely polarized targets, and the HERMES data clearly show that the quark transversity distribution is indeed non-zero.

When quark intrinsic transverse momentum (k_T) is taken into account, the description of quarks in a nucleon involves a set of 8 transverse momentum dependent (TMD) distributions at leading order [3], as illustrated in Fig. 1. The gauge invariant definitions of TMD and factorization theorems for polarized SIDIS were carefully studied by Ji, Ma and Yuan [4] and by Collins and Metz [5]. Of the 8-TMDs, six are time reversal even and two are time reversal odd ($f_{1T}^{\perp}$ and $h_1^{\perp}$), three of them survive the integration over k_T and produce the regular distribution functions with $g_{1L} \to g_1$ and $h_{1T} \to h_1$. Among the other five TMDs, so far, only the Sivers function $f_{1T}^{\perp}$ has been experimentally verified as non-vanishing [1]. There has been some indication from Drell-Yan cross sections and SIDIS cross sections that the Boer-Mulders function [6] $h_1^{\perp}$ might also be non-vanishing.

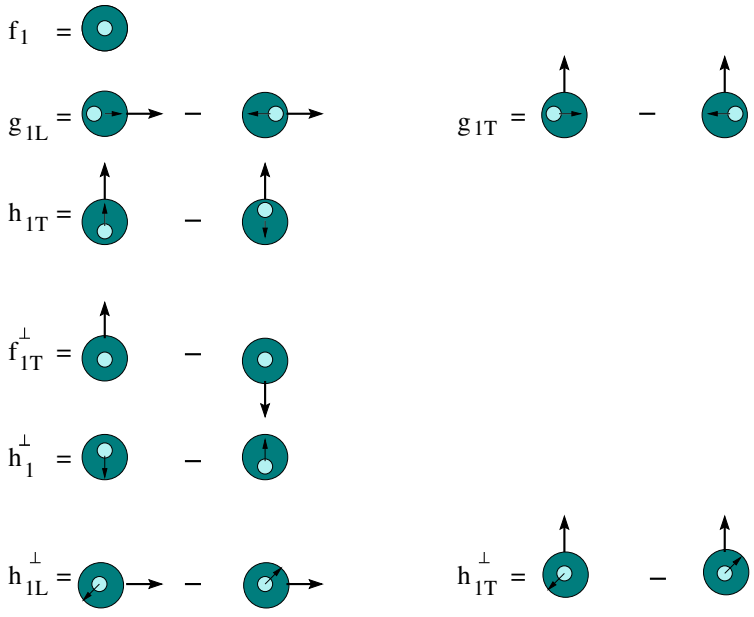

Figure 1: An illustration of 8 transverse momentum dependent quark distribution functions.

The goal of this experiment is to make the first definitive measurement of the quark transverse momentum dependent distribution g_{1T} and to clearly establish if it is non-zero. The distribution function, g_{1T}^q, describes longitudinal polarization of quarks in the transversely polarized nucleon, it is non-vanishing only with the existence of a non-zero quark transverse momentum k_T, thus a non-zero quark angular momentum. The longitudinal polarization of the active quark, g_{1T}, leads to a double spin asymmetry (longitudinally polarized lepton and transversely polarized target nucleon), $\mathcal{A}_{LT}$. With the fast helicity flip of Jefferson Lab's highly polarized electron beam, this type of double-spin asymmetry $\mathcal{A}_{LT}$ is one of the clearest and easiest experimental observables one can measure in SIDIS reactions at JLab.

On the theory side, there have been several calculations of g_{1T} based on a spectator model [7] and a Bag Model [8]. Both models predict opposite behavior between the u-quark and d-quark, similar to that of g_1, and both calculations predict an asymmetry $\mathcal{A}_{LT}$ at the level of $5\% \sim 10\%$ at JLab kinematics for $p(e, e'\pi^+)$ reactions. In addition, Mulders *et. al.* established the *Lorentz invariance relation* [3] between the first k_T-momentum of g_{1T}^q and the distribution function $g_2^q(x)$, namely:

$$g_2^q(x) = \frac{d}{dx} g_{1T}^{q\,(1)}(x). \tag{1}$$

Following this relation, Kotzinian *et. al* [9] calculated $g_{1T}^{q(1)}$ and predicted $\mathcal{A}_{LT}$ to be $8\% \sim 10\%$ at the kinematics of this experiment.

However, recent theory developments have shown that the gauge link entering into the definitions of distribution functions plays an important role. For example, it allows a non-zero Sivers distribution function $f_{1T}^{\perp}$ to exist [10]. At first some model calculations, and after that general considerations, demonstrated [11,12,13] that the Lorentz invariance relation suggested by Mulders *et. al.* can be violated due to the presence of the gauge link. To clearly establish experimentally the importance of the QCD gauge link, and thus the violation of Lorentz invariance relation, one can make a definitive measurement of $\mathcal{A}_{LT}$ and demonstrate its deviation from the predictions which follow the Lorentz invariance relation, such as that of Kotzinian *et. al.* This is the basic approach of this experiment.

2 Physics motivations

2.1 Semi-Inclusive DIS cross section and asymmetry $\mathcal{A}_{LT}$

The kinematics and the coordinate definition are illustrated in Fig. 2. We define E′ as the energy of the scattered electron and θ_e is the scattering angle, $\nu = E - E'$ is the energy transfer. The Bjorken-x, which indicates the fractional momentum carried by the struck quark, is defined as: $x = Q^2/(2\nu M_N)$, M_N is the nucleon mass. The momentum of the outgoing hadron is p_h and the fraction of the virtual photon energy carried by the pion is: $z = E_h/\nu$. The hadron transverse momentum relative to $\vec{q}$ is labeled as $P_{h\perp}$. At the leading order, when h is a spin zero particle,

the SIDIS cross section[3,6] can be expressed as:

$$
\begin{aligned}
d^6\sigma^{LO} = \frac{d\sigma^{\ell+N\to\ell'+h+X}}{dx dy d\phi^\ell dz d^2\boldsymbol{P}_{h\perp}} = \frac{4\pi\alpha^2\, s\, x}{Q^4} \times \\
\Bigg\{ \left(1 - y + \frac{y^2}{2}\right) \sum_q e_q^2\, f_1^q \cdot D_1^q \\
+ (1-y)\, \cos(2\phi_h^\ell) \sum_q e_q^2 \left[\frac{P_{h\perp}^2}{4z^2 M_N\, M_h} h_1^{\perp q} \otimes H_1^{\perp q}\right] \\
- |\boldsymbol{S}_L|\, (1-y)\, \sin(2\phi_h^\ell) \sum_q e_q^2 \left[\frac{P_{h\perp}^2}{4z^2 M_N\, M_h} h_{1L}^{\perp q} \otimes H_1^{\perp q}\right] \\
+ |\boldsymbol{S}_T|\, (1-y)\, \sin(\phi_h^\ell + \phi_S^\ell) \sum_q e_q^2 \left[\frac{P_{h\perp}}{z M_h} h_1^q \otimes H_1^{\perp q}\right] \\
+ |\boldsymbol{S}_T| \left(1 - y + \frac{1}{2}\, y^2\right) \sin(\phi_h^\ell - \phi_S^\ell) \sum_q e_q^2 \left[\frac{P_{h\perp}}{z M_N} f_{1T}^{\perp q} \otimes D_1^q\right] \\
+ |\boldsymbol{S}_T|\, (1-y)\, \sin(3\phi_h^\ell - \phi_S^\ell) \sum_q e_q^2 \left[\frac{P_{h\perp}^3}{6z^3 M_N^2\, M_h} h_{1T}^{\perp q} \otimes H_1^{\perp q}\right] \\
+ \lambda_e\, |\boldsymbol{S}_L|\, y\, (1 - \frac{1}{2}\, y) \sum_q e_q^2\, g_1^q \cdot D_1^q \\
+ \lambda_e\, |\boldsymbol{S}_T|\, y\, (1 - \frac{1}{2}\, y)\, \cos(\phi_h^\ell - \phi_S^\ell) \sum_q e_q^2 \left[\frac{P_{h\perp}}{z M_N} g_{1T}^q \otimes D_1^q\right] \Bigg\}. \qquad (2)
\end{aligned}
$$

where $|\boldsymbol{S}_L|$ and $|\boldsymbol{S}_T|$ are the longitudinal and transverse target spin component, λ_e is the electron helicity. The azimuthal angles ϕ_h and ϕ_S are defined according to the Trento conventions[14] as shown in Fig. 2.

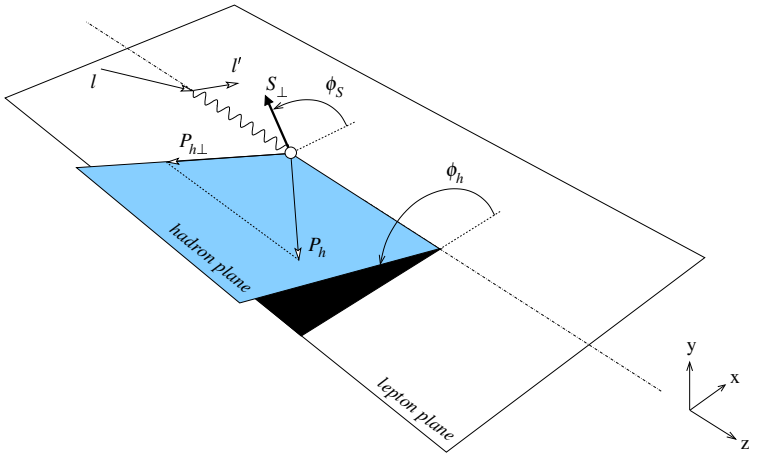

Figure 2: The definition of ϕ_h and ϕ_S according to the Trento conventions.

The convolution in Eq. 2 represents an integration over transverse momentum of

initial ($\mathbf{k_T}$) and final quark ($\mathbf{p_T}$) with proper weighting [15], i.e.

$$[.. \otimes ..] = \int d^2\mathbf{p_T} d^2\mathbf{k_T} \delta^{(2)}(\mathbf{p_T} - \frac{\mathbf{P_{h\perp}}}{z} - \mathbf{k_T})[...]. \tag{3}$$

These convolutions can be reduced to simple products if the $|P_{h\perp}|$-weighted integrations are taken or explicit $\mathbf{p_T}$ and $\mathbf{k_T}$ dependencies (like Gaussian distributions) are introduced.

Only the last term in Eq. 2 is related to both beam helicity and transverse target spin, the corresponding double-spin asymmetry is:

$$\mathcal{A}_{LT}(x,y,z) \equiv \frac{\sigma_{LT}}{\sigma_{UU}} = \frac{y(1-\frac{1}{2}y)}{1-y+\frac{y^2}{2}} \cdot \frac{\sum_q e_q^2 \left[\frac{P_{h\perp}}{zM_N} g_{1T}^q \otimes D_1^q\right]}{\sum_q e_q^2 f_1^q D_1^q} \tag{4}$$

Following the definition of Kotzinian *et. al* [9], we include the kinematic factor $\mathcal{D}(y) = y(1-\frac{1}{2}y)/(1-y+\frac{1}{2}y^2)$ in $\mathcal{A}_{LT}$. In the kinematics of this experiment we have $\mathcal{D}(y) = 0.87 \sim 0.97$.

2.2 Model calculations of g_{1T}^q.

There has been several model calculations of g_{1T}. In addition to what listed below, another calculation of a revised version of Gamberg *et al.* [16] will be available in January 2007.

Spectator model

In a simple spectator model, Jacob, Mulders and Rodrigues [7] calculated the first k_T moment $g_{1T}^{q(1)}$ which is defined as:

$$g_{1T}^{q\,(1)}(x) = \int d^{\,2}k_T \, \frac{\mathbf{k_T^2}}{2M^2} \, g_{1T}^q(x, k_T^2). \tag{5}$$

As shown in Fig. 3, this model predicted opposite behavior of g_{1T}^q between u-quark and d-quark, following that of g_1^q as expected. In comparison, the quark momentum distribution xf_1 generated from the same model is also shown. The ratio for u-quark $g_{1T}^{u(1)}/f_1^u$, which sets the magnitude for $\mathcal{A}_{LT}$ in $p(e,e'\pi^+)$, is about 5%.

Bag model

F. Yuan calculated $g_{1T}^{q(1)}$ together with the other TMDs in a Bag Model [8], and the ratio $g_{1T}^{q(1)}/f_1^q$ are shown in Fig. 4. The basic features of this calculation are similar to those of Jacob *et. al* with the d-quark's effect being opposite to that of the u-quark and about half the size.

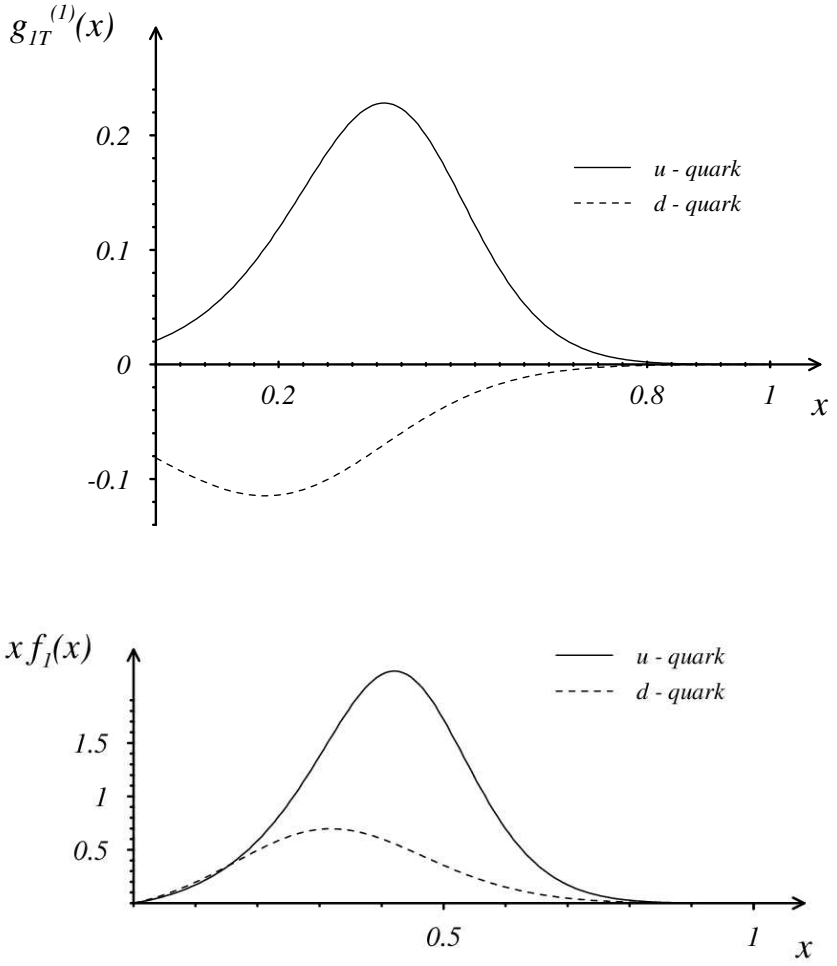

Figure 3: Model calculation of $g_{1T}^{q(1)}(x)$ (top panel) for u-quark and d-quark of Jacob, Mulders and Rodrigues. At the bottom panel, the quark distribution $xf_1^q(x)$ are plotted from the same model. At $x = 0.4$ for example, this model predicted $g_{1T}^{u(1)}/f_1^u \approx 0.05$.

Lorentz invariance relation

As is shown by Mulders and Tangerman [3], $g_{1T}^{q(1)}(x)$ is related to the distribution function $g_2^q(x)$,

$$g_2^q(x) = \frac{d}{dx}\, g_{1T}^{q(1)}. \tag{6}$$

This relation arises from constraints imposed by Lorentz invariance on the antiquark-target forward scattering amplitude and the use of QCD equations of motion for quark fields [3]. There has been a reasonable DIS experiment data set to extract information on $g_2^q(x)$ or, one can use the Wandzura and Wilczek [17] approximation

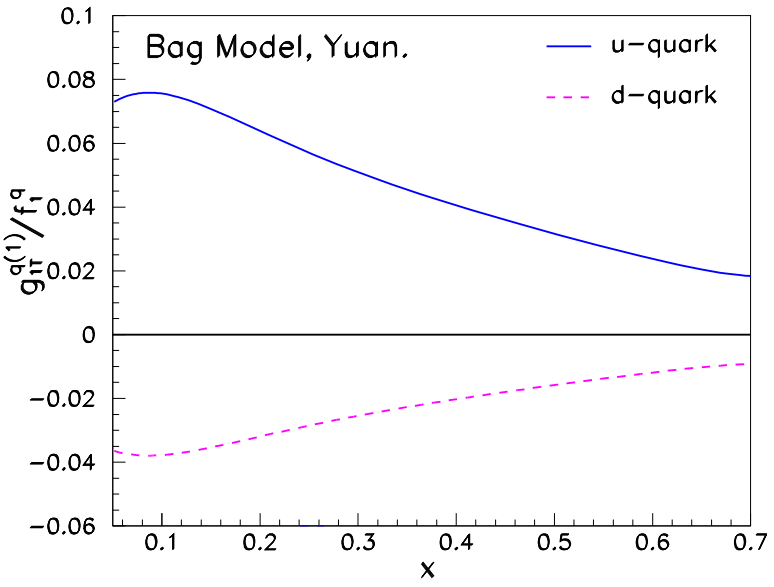

Figure 4: The ratio of $g_{1T}^{q(1)}(x)/f_1^q(x)$ for u-quark and d-quark from a Bag Model calculation of F. Yuan [8].

for $g_2^q(x)$

$$g_2^q(x) \approx -g_1^q(x) + \int_x^1 dy \, \frac{g_1^q(y)}{y}, \tag{7}$$

and follow the relation [18]:

$$g_{1T}^{q(1)}(x) \approx x \int_x^1 dy \, \frac{g_1^q(y)}{y}. \tag{8}$$

Kotzinian *et al.* [9] estimated the ratio $g_{1T}^{q(1)}(x)/f_1^q(x)$ using the leading order GRV98 [19] unpolarized and corresponding GRSV2000 [20] polarized distribution functions, the results are shown in Fig. 5. The asymmetry $\mathcal{A}_{LT}$ at the JLab 6 GeV kinematics of this experiment are predicted, at our request, using the above ratio and the Kretzer [21] fragmentation functions, as shown in Fig. 6 for its dependence on x, $y = \nu/E$ and $z = E_\pi/\nu$. As expected, the $\mathcal{A}_{LT}$ asymmetry is the largest in $p(e, e'\pi^+)$ reaction, at the level of $8\% \sim 10\%$.

The violation of Lorentz invariance relation

Recently, it has been shown that gauge link in the definitions of distribution functions plays a important role, for example, it provides the possibility for non-zero Sivers effect [10]. Although it is still an on-going debate, it was demonstrated [11,12,13]

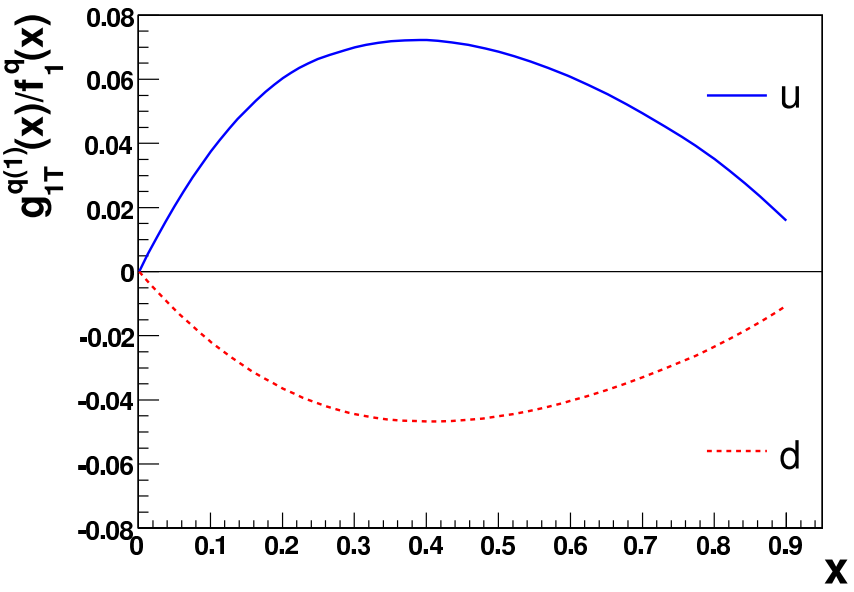

Figure 5: The ratio $g_{1T}^{q(1)}(x)/f_1^q(x)$ for u-quark and d-quark from Kotzinian *et al*[9] at $Q^2 = 2.0$ GeV^2.

that the Lorentz invariance relation suggested by Mulders *et. al.* can be violated due to the presence of the gauge link.

How important a role does the QCD gauge link play? How much violation is the Lorentz invariance relation? Through a definitive measurement of $\mathcal{A}_{LT}$, we expect to have a clear answer when data from this experimental is confronted with the predictions which follow the Lorentz invariance relation, such as that of Kotzinian *et. al.*

2.3 u-quark dominance in SIDIS $p(e, e'\pi^+)$ reaction

In the SIDIS reaction of $p(e, e'\pi^+)$, the u-quark contribution dominates the cross section. At large enough z_π, the favored fragmentation function is much larger than the unfavored fragmentation function i.e. $D^+(z) > D^-(z)$, further enhance the u-quark dominance. The contribution of quark flavor q to the total SIDIS cross section is:

$$\frac{\sigma_q}{\sigma_{all}} = \frac{e_q^2 f_1^q(x) \cdot D_1^q(z)}{\sum_i e_i^2 f_1^i(x) \cdot D_1^i(z)} \tag{9}$$

As shown in Figure 7, u-quarks make up 90% $\sim$ 95% of the total cross section. In K^+ production, u-quark contribution also dominates. Under the condition of u-quark dominance, we have:

$$[A_{LT}(x,z)]_p^{\pi^+} \propto \frac{g_{1T}^{u(1)}(x)}{f_1^u(x)}. \tag{10}$$

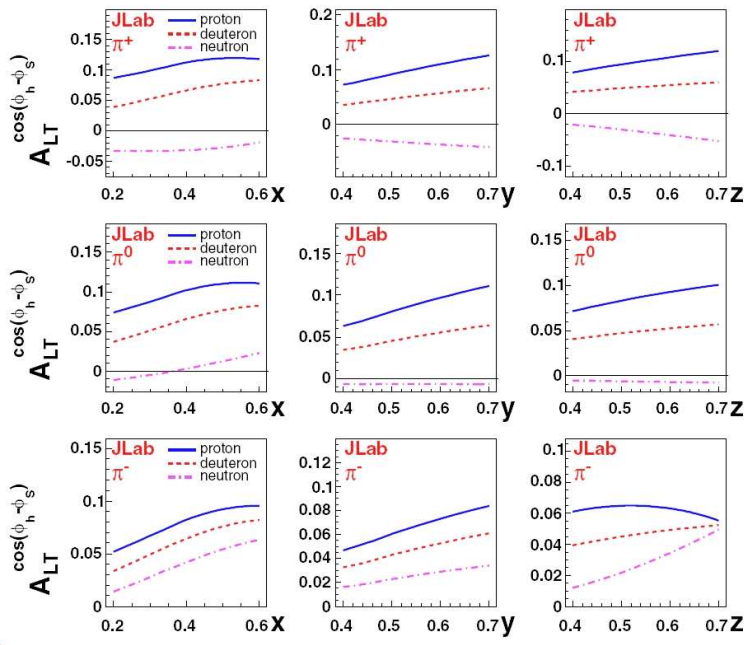

Figure 6: Predictions of $\mathcal{A}_{LT}$ by Kotzinian *et al.*[9] at JLab 6 GeV energy for SIDIS production of π^+ (top panels), π^0 (middle panels) and π^- (bottom panels) on proton (solid lines), deuteron (dashed lines) and neutron (dot-dashed lines).

2.4 Experimental observables

From Eq. 2, in order to access the quark transverse momentum dependent distribution g_{1T} one needs to have longitudinally polarized lepton beam scatter on a transversely polarized target and form asymmetry $\mathcal{A}_{LT}$. In practice, there are two ways of measuring $\mathcal{A}_{LT}$ thus extracting g_{1T}:

- Form the $\cos(\phi_h - \phi_S)$ moment of the SIDIS cross section corresponding to a fixed beam helicity and target transverse spin direction.

- Form the asymmetry $\mathcal{A}_{LT}$ with a fixed target transverse spin direction while flipping the lepton beam helicity.

In this experiment, we follow the second approach, taking the full advantage of the fast helicity flip of CEBAF's polarized electron beam. The acceptance of this experiment is centered around $\phi_h = 180°$, $\phi_S = 0°$ for target spin pointing to BigCal side and $\phi_S = 180°$ for target spin pointing away from BigCal side, perfect for measuring the double-spin asymmetries at the maximum value of $\cos(\phi_h - \Phi_S)$.

The direct experimental observed asymmetries, for target spin pointing to the BigCal side, will be formed as:

$$[\mathcal{A}_{LT}(\phi_S = 0°)]_{meas} = \frac{N(\lambda_e = 1, \phi_S = 0°) - N(\lambda_e = -1, \phi_S = 0°)}{N(\lambda_e = 1, \phi_S = 0°) + N(\lambda_e = -1, \phi_S = 0°)} \qquad (11)$$

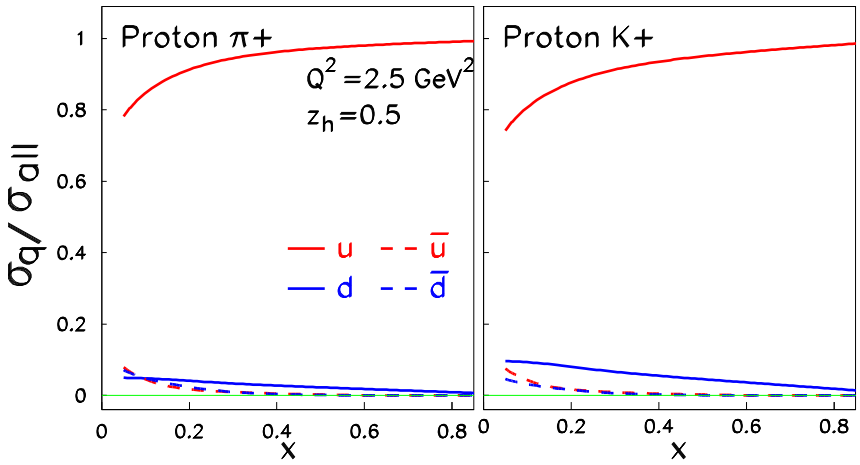

Figure 7: The ratio of SIDIS cross section from each quark flavor (σ_q) to the total SIDIS cross section (σ_{all}) corresponding to the kinematics of this experiment in $p(e,e'\pi^+)$ (left) and $p(e,e'K^+)$ (right) reactions.

and for the case of target spin pointing away from the BigCal side:

$$[\mathcal{A}_{LT}(\phi_S = 180^\circ)]_{meas} = \frac{N(\lambda_e = 1, \phi_S = 180^\circ) - N(\lambda_e = -1, \phi_S = 180^\circ)}{N(\lambda_e = 1, \phi_S = 180^\circ) + N(\lambda_e = -1, \phi_S = 180^\circ)} \tag{12}$$

Compared with the physics asymmetries $\mathcal{A}_{LT}$, the measured asymmetries are diluted by the existence of unpolarized nucleons in the target (thus dilution factor f^{π^+}), the fact that neither the beam nor the target are 100% polarized, i.e.:

$$\mathcal{A}_{LT} = \frac{(\mathcal{A}_{LT})_{meas}}{f^{\pi^+} P_B P_T} \tag{13}$$

We follow the notation of Kotzinian *et al.* which included the lepton kinematic factor $\mathcal{D}(y)$ in the definition of asymmetry $\mathcal{A}_{LT}$. One expects a sign change corresponding to a target spin-flip, i.e.: $\mathcal{A}_{LT}(\phi_S = 0^\circ) = -\mathcal{A}_{LT}(\phi_S = 180^\circ)$.

3 The Experiment

The technical details of this experiment is mostly identical to that of the approved "semi-SANE" [22] (E04-113) and "SANE" [23] (E03-109) experiments. The large acceptance *BETA* detector, in the identical setting as in the SANE experiment, will be used to detect the scattered electrons at 40°. The HMS spectrometer will be used to detect π^+ at 2.3 GeV/c and 14° in coincidence ($z_\pi \approx 0.5$). The standard Hall C polarized NH_3 target will be used in its transverse setting identical to that of the SANE experiment. The trigger of this experiment will be a coincidence between the HMS-single and the calorimeter-single of *BETA*.

3.1 The choice of kinematics

The definitions of the kinematic variables are the following: Bjorken-x, which indicates the fractional momentum carried by the struck quark, is $x = Q^2/(2\nu M_N)$, where M_N is the nucleon mass. The momentum of the outgoing pion is p_π and the fraction of the virtual photon energy carried by the pion is: $z_\pi = E_\pi/\nu$. W is the invariant mass of the whole hadronic system and W' is the invariant mass of the hadronic system without the detected hadron. We have:

$$W^2 = M_N^2 + Q^2(\frac{1}{x} - 1),$$
$$W'^2 = (M_N + \nu - E_\pi)^2 - |\vec{q} - \vec{p}_\pi|^2. \quad (14)$$

We chose to cover the highest possible W with a 6 GeV beam, $2.2 < W < 3.0$ GeV, corresponds to $0.21 < x < 0.53$ and $2.0 < Q^2 < 4.4$ (GeV/c)^2. We also chose to detect the leading fragmentation pion which carries $z_\pi \approx 0.5$ of the energy transfer to favor current fragmentation. The value of W' is also chosen to be as high as possible with a cut of $W' > 1.6$ GeV to avoid contributions from resonance production channels. The kinematics for each x-bin center are listed in Table 1. Because the BigCal detector can take electron with a large momentum range, only one setting is needed to cover all the kinematics listed in Table 1. The hadron arm momentum will be set to $p_\pi = 2.3$ GeV/c, and the corresponding values of the missing mass W' and z_π are listed in Table 1.

Table 1: Nominal kinematics of each x-bin center for beam energy of $E = 6.0$ GeV. One BigCal+HMS setting covers all the kinematics listed. E$'$ and θ_e are the electron arm momentum and angle. θ_q indicates the direction of $\vec{q}$. The hadron arm angle is fixed at 14°.

E$'$ GeV	θ_e deg.	$\langle x \rangle$	W GeV	Q^2 GeV^2	θ_q deg.	z_π	p_π GeV/c	W' GeV
						$\theta_\pi = 14.0°$		
0.725	40.0	0.206	2.957	2.035	4.89	0.44	2.30	2.22
1.150	40.0	0.355	2.599	3.229	8.22	0.48	2.30	1.94
1.575	40.0	0.533	2.182	4.422	11.93	0.52	2.30	1.61

As shown in Fig. 8, the HMS spectrometer will be located at 14° beam right as the hadron arm detector. It will be set at a central momentum of 2.3 GeV/c in positive polarity. For the electron arm, we will use a combination of a large calorimeter (*BigCal*), lucite array and gas Cherenkov. This is the same detector package that will be used in the two approved experiment [23] E03-109," Spin Asymmetries on the Nucleon Experiment" (SANE) and E04-113 " Semi-Inclusive Spin Asymmetries on the Nucleon Experiment" (semi-SANE). This electron detector, the Big Electron Telescope Array (*BETA*), will be centered at 40° on beam left, identical to the setting of SANE experiment. A detailed description and update of *BETA* detector

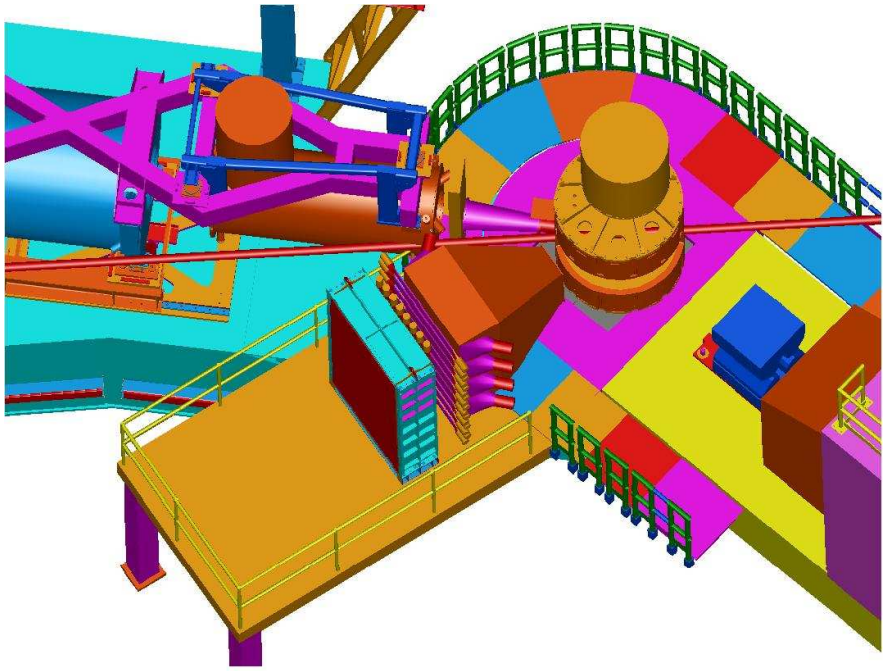

Figure 8: A top view of the floor arrangement of this experiment, which is very similar to that of SANE and semi-SANE experiments. The thick red line represents the beam which is incident from the right (the beam dump is to the left of the picture). The electron-arm detector (*BETA*) , with *BigCal* in the back, the gas Cherenkov in the front and the lucite array in between, is at 40° beam left. The HMS is at 14° beam right. The SOS spectrometer will be parked at a backward angle on beam left.

is given in the SANE experiment's PAC31-update. Unlike the SANE experiment, which takes single-arm electrons in *BETA*, this experiment is a coincidence $p(e, e'\pi^+)$ measurement, and the HMS can be used for target position reconstruction. From coincidence timing and HMS vertex cuts one can easily eliminate the majority of the background events in *BETA*, which has been a major technical concern for the SANE experiment.

3.2 The electron detector BETA

The electron detector, *BETA*, will be the same as will be used in the SANE experiment. Details of *BETA* are given in the SANE experiment proposal and its jeopardy update to PAC31. A brief overview of *BETA* is given here. One main component of *BETA* is a large lead glass calorimeter array, *BigCal*, to measure the energy of the electrons. *BigCal* has been assembled by the Hall C G_{Ep} collaboration. *BigCal* will first be used in experiments E04-108 and E04-013 scheduled to run in 2007. For SANE experiment, *BigCal* will be augmented with three new detectors to become the Big Electron Telescope Array, *BETA*. For the SANE experiment and this experiment the main new detector is a segmented threshold gas Cherenkov for additional π/e separation. A pion rejection factor of 1000:1 is expected by the combination of BigCal and the gas Cherenkov. SANE plans to use two hodoscopes: one near the target and one between the Cherenkov and the calorimeter. These hodoscopes allow tracking back to the target to reduce beam related background. For this experiment, the hodoscopes are not necessary, since target reconstruction and cuts will be done using the HMS spectrometer.

The calorimeter array, *BigCal*, combines lead-glass blocks used in the Hall A Real Compton experiment with lead-glass from the Protvino group that was used at Fermilab. Each RCS lead-glass block has a 4x4 cm cross-section and length of 40 cm, while the Protvino lead-glass block has 3.8x3.8 cm cross-section with a length of 45 cm. The lead-glass is being stacked 218 cm in height x 120 cm in width, forming a solid angle of 210 msr at a distance of 3.5 meter from the target. The blocks are individual wrapped with a thin layer of 1 mil thick aluminized mylar so that they are optically isolated from each other. The electron energy resolution is expected to be $5\%/\sqrt{E(\mathrm{GeV})}$. A horizontal and vertical position can be determined by the energy-weighted centroid of the cluster of blocks which share the energy and is expected to be better than 0.5 cm. For coincidence events, the target position will be determined by the HMS to about 0.5 cm so that expected angular resolution for the scattered electron is about 3 mrad. We propose to use the technique of π° mass reconstruction as a means of calibration. This technique has been used in other experiments, such as the RadPhi experiment (E94-016) at JLab and E852 at Brookhaven which employed a large calorimeter. The gain monitoring system will be designed and constructed by the University of Virginia group based on the gain monitoring system that they successfully implemented for the RadPhi experiment.

Temple University has designed and is constructing a gas Cherenkov detector for

SANE experiment. The gas Cherenkov will have a length of 164 cm with the radiator gas occupying a length of 125 cm. A total of eight mirrors will be employed in two columns of 4. The mirrors are designed for point-to-point focusing from the target cell to the photomultiplier tube. The gas Cherenkov will use dry N_2 gas which at 20° C has an index of refraction of 1.000279. This corresponds to a pion momentum threshold of 5.9 GeV/c. The expected number of photo-electrons is 17∼20. For a single-arm inclusive experiment, such as SANE, a gas Cherenkov detector is critical for the rejection of pion background. However, for a coincidence experiment, such as this experiment, particle ID contamination on the electron-arm side can be mostly eliminated by a cut on coincidence time-of-flight.

3.3 The hadron detector: HMS

This experiment will have the HMS spectrometer set in positive polarity, at an angle of 14° and at a central momentum of 2.3 GeV/c. Protons in HMS, which take 6 ns longer flight time than π^+, can be easily ruled out through coincidence time-of-flight cuts. In addition, the present HMS aerogel detector , which has an aerogel with n = 1.030, will fire for π^+ and K^+ but not proton. The separation of K^+ from π^+ is not critical in this experiment due to several reasons: first, at 2.3 GeV/c the Kaon survival factor is 0.23 result in a K^+ rate $\sim$ 10% of that of π^+, second, as have been shown in HERMES data, the production of K^+ is strongly dominated by u-quark in SIDIS just as in π^+ production, thus the small contamination of K^+ does not ruin the physics interpretation of $[\mathcal{A}_{LT}]_p^{\pi^+}$ in this experiment. At a momentum of 2.3 GeV/c, charged Kaons barely cross the Cherenkov threshold of the aerogel detector, a cut on the number of photo-electrons from the aerogel will reduce the K^+ contamination.

3.4 Trigger, time-of-flight resolution and background rates

The hadron trigger in the HMS will be the standard coincidence of 3 out of 4 scintillator planes. The electron arm trigger will be the coincidence of the gas Cherenkov and the calorimeter. The hardware threshold for the Cherenkov trigger will be 0.5 to 1 photoelectrons. For the calorimeter, the analog signals from the individual blocks will be summed in groups of eight to produced a summed signal plus the individual analog signals are passed through to an ADC. The summed analog signal will be sent to a discriminator and a threshold equivalent to depositing 500 MeV in the calorimeter will be set. This logical signal will be sent to a TDC. In addition, it will be used as part of a coincidence circuit for the electron arm trigger and eventually for the coincidence between the hadron and electron arms.

To calculate singles rates in the electron arm , a Monte Carlo simulation which includes the target field, the geometry of the target and the magnet's coils was developed by Dr. G. Warren. Rates for electrons, positrons, charge pions, protons and neutrons were calculated. Different codes were incorporated into the Monte

Carlo for the different particle types. The strong 5T target holding field forces low energy charge particles to the direction of the beam. From the Monte Carlo, it is expected that charged particles must have a momentum greater than 180 MeV/c in order to reach the electron arm when it is centered at 40°. The expected trigger rates for different particle types are given in Table 2. The rates in the Cherenkov detector are calculated assuming a threshold of 0.5 to 1 photo-electron which reduces the raw rate of charged pions by a factor of 100 and essentially eliminates the protons and neutrons. The rates in the calorimeter were calculated assuming a 500 MeV threshold on the energy deposited in the calorimeter.

Based on the individual detector rates given in Table 2, We expected the rate of true coincidence between the gas Cherenkov and the calorimeter to be 0.39 KHz with an additional accidental rate of 0.07 KHz. The singles rate in the HMS will be below 10 KHz. With a 100 ns coincidence window between the electron arm and the HMS the accidental coincidence rate will be below 1 Hz for the whole 100 ns window. These accidentals can be further reduced by a factor of 10 by a higher cut on the number of photo-electrons in the data analysis and then additional factor of 20 by a 5 ns cut on the coincidence time. The final accidental rate should be less than 0.002 Hz with the timing cut.

	Cherenkov			Calorimeter			
Particle type	e^++e^-	π^++π^-	Trigger	e^++e^-	π^++π^-	π^0+p+n	Trig
Rate (KHz)	1.2	236	3.6	0.3	11.5	79.8	91.6

Table 2: The expected rates for a trigger in the Cherenkov or the calorimeter under assumptions given in the text.

The coincidence time resolution will be dominated by the timing resolution of the lead glass blocks in BigCal. Experiment 99-007 in Hall A studied the elastic ep reaction using a lead glass array with a much larger block size to detect electrons in coincidence with protons which were detected in the Hall A HRS. In Fig. 9, the coincidence time spectra for Hall A experiment E99-007 is shown. The resolution in coincidence time has a 3σ of about 3.5 ns. For momentum around 2.3 GeV/c the time-of-flight difference between the protons and kaons is larger than 3.5 ns .

4 Monte Carlo simulations and phase space coverage

The phase space coverage is obtained from a detailed Monte Carlo simulation which includes realistic HMS spectrometer models as well as target and detector geometry. The coverage in the (Q^2, x) and (W, x) planes is shown in Fig. 10, and the coverage in the (W', x), $(P_\perp, x)$ and (z_π, x) planes is shown in Fig. 11, color coded for each x-bin.

The angular coverage of ϕ_h^l and ϕ_S^l is shown in Fig. 12 and Fig. 13. Two settings of target spin orientation will be taken with $\langle\phi_S^l = 0°$ and 180°. The coverage of the

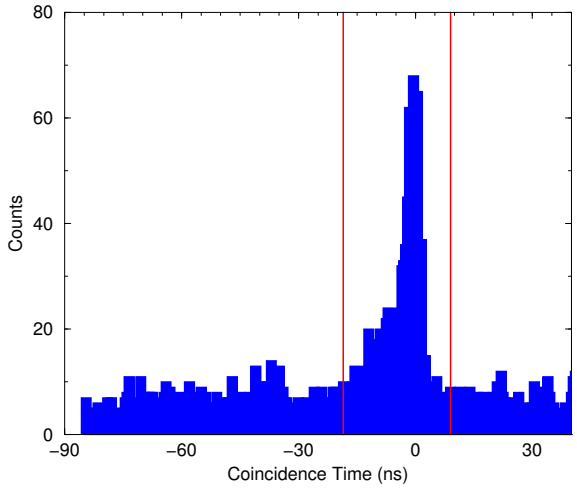

Figure 9: Typical coincidence time-of-flight (TOF) spectra of ep elastic scattering in E99-007. The tail to negative TOF is walk in the TDC time due to smaller ADC pulses in the lead glass block. This could have been corrected for, but for the purposes of 99-007 experiment the resolution was adequate.

"Sivers angle" $\phi_h - \phi_S^l$ angle is shown in Fig. 14. For each x-bin in this experiment, the full 2π range of the Collins angle $\phi_h + \phi_S^l$ is covered. as shown in Fig. 15.

5 Event Rate Estimate and Projected Uncertainties

5.1 Cross section and rate estimate

The estimation of the coincidence cross sections has the following inputs:

- The inclusive $p(e, e')$ cross sections. Deep-inelastic cross section of ^{14}N are assumed to be the sum of the protons and the neutrons, neglecting the nuclear effects.
- Parameterizations of the fragmentation functions D_π^+ and D_π^-.
- A model of the transverse momentum distributions of pion and kaon as fragmentation products.

The inclusive deep inelastic (e, e') cross section can be expressed in the quark parton model as:

$$\frac{d^2\sigma}{d\Omega dE'} = \frac{\alpha^2(1+(1-y)^2)}{sxy^2}\frac{E'}{M_N\,\nu}\sum_{q,\bar{q}} e_q^2 f_1^q(x), \tag{15}$$

where $s = 2E\,M_N + M_N^2$. The unpolarized quark distribution functions $f_1^q(x)$ and $f_1^{\bar{q}}(x)$ are taken from the CTEQ global fits [24]. The semi-inclusive $(e, e'h)$ cross

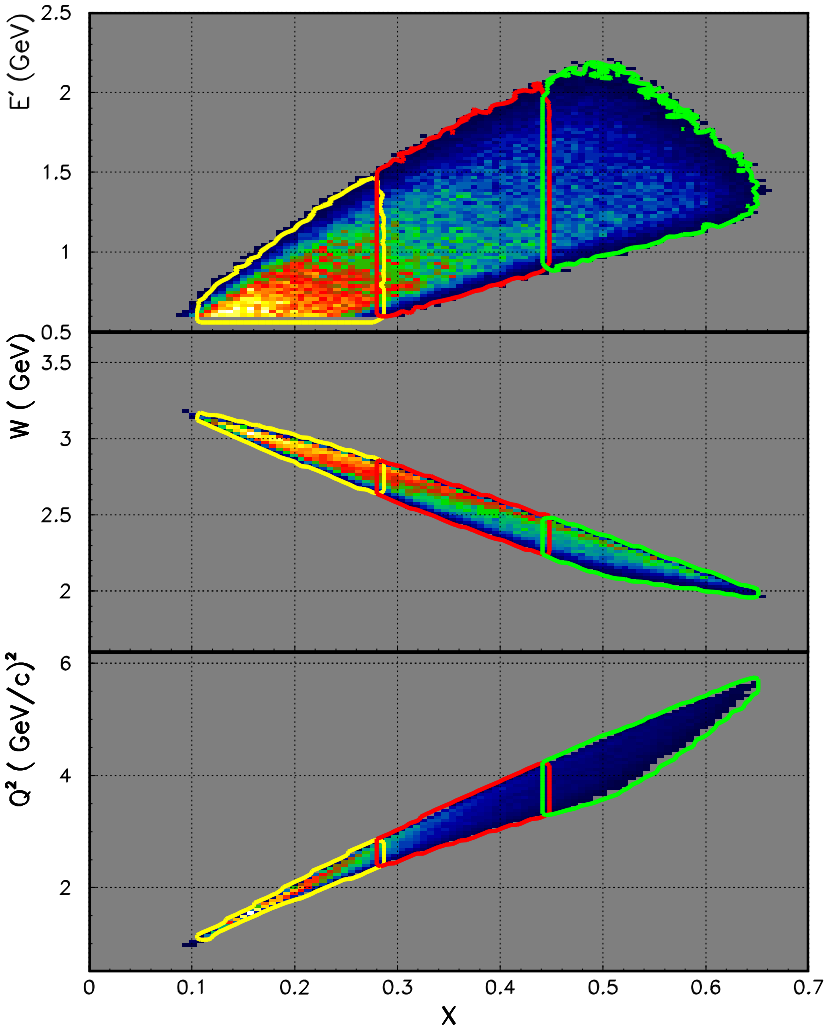

Figure 10: Available phase space in the (Q^2, x) and (W, x) planes with each x-bin in different colors.

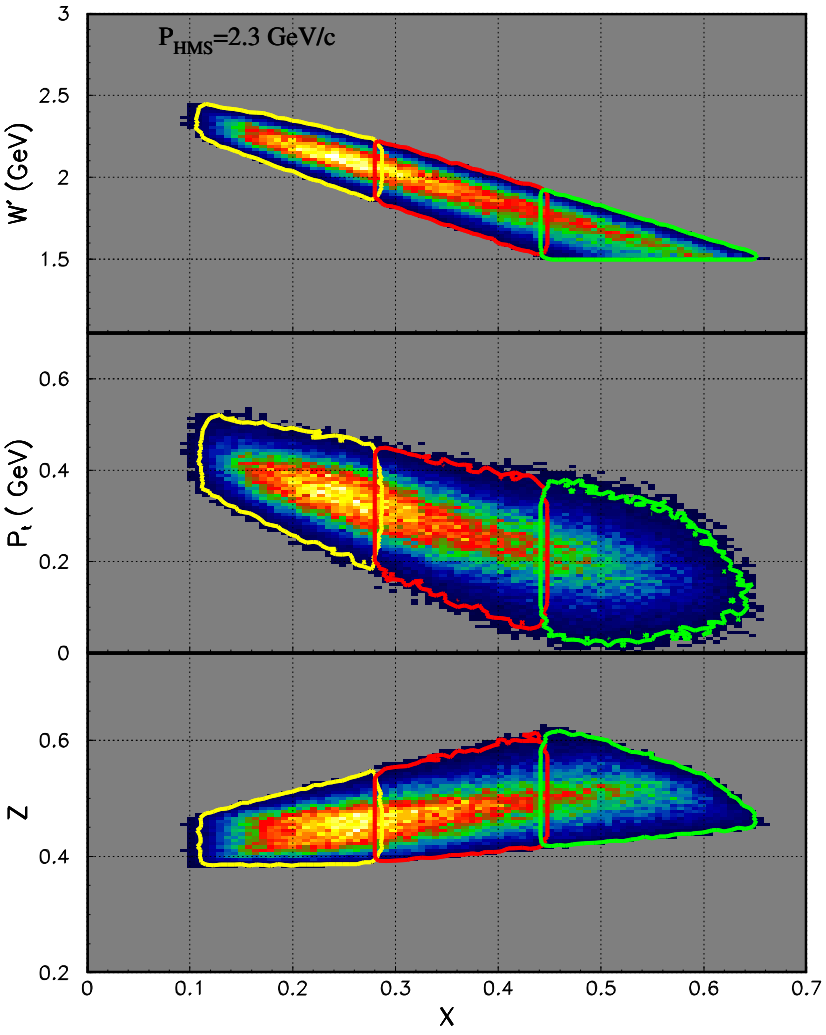

Figure 11: Same as in Fig. 10, phase space coverage in (W', x), $(P_\perp, x)$ and (z_π, x)

.

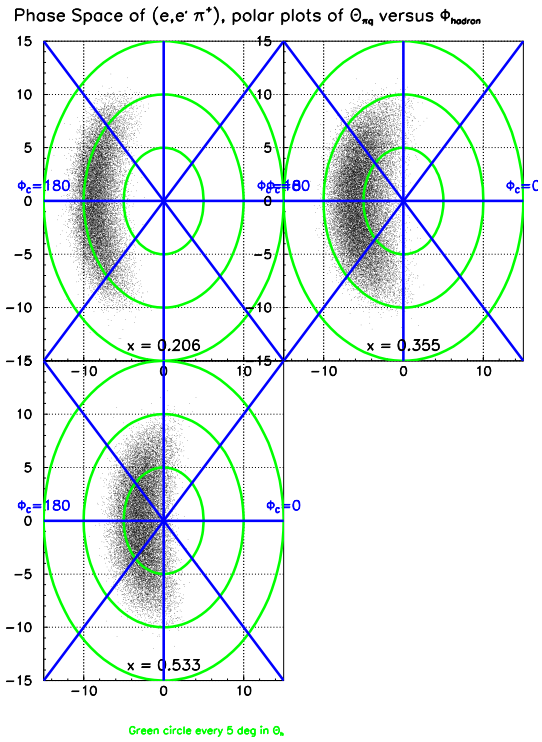

Figure 12: Angular coverage of ϕ_h^l are shown for each x-bin, viewed along $\vec{q}$.

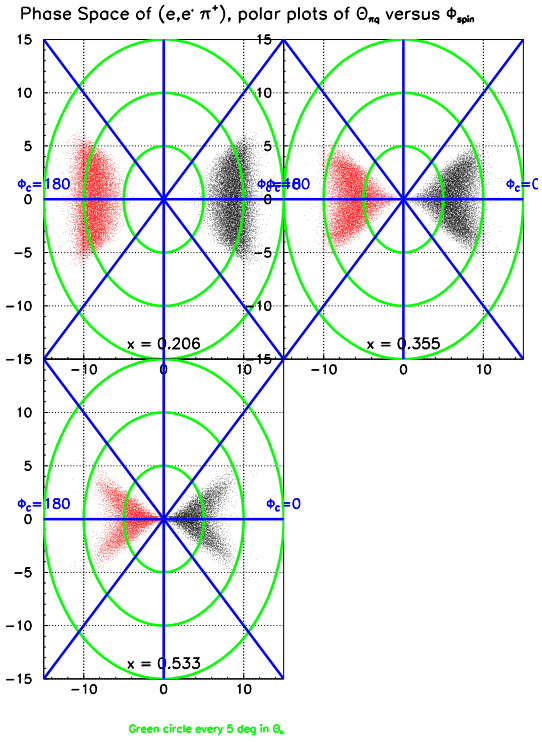

Figure 13: Angular coverage of ϕ_S^l are shown for each x-bin, viewed along beam. Black: $\phi_S^l = 0°$. red: $\phi_S^l = 180°$.

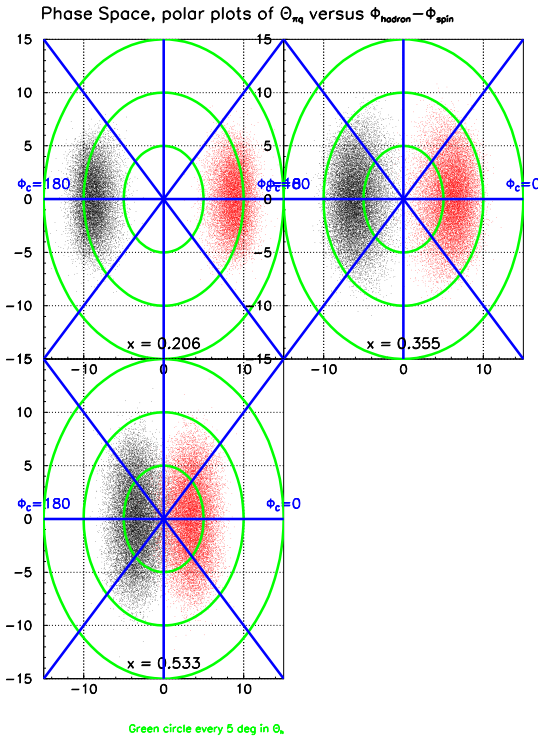

Figure 14: Angular coverage of $\phi_h - \phi_S^l$ are shown for each x-bin, viewed along beam. Black: $\phi_S^l = 0°$. red: $\phi_S^l = 180°$.

section relates to the quark fragmentation function $\mathrm{D}_q^h(z)$ and the total inclusive cross section σ_{tot} through:

$$\frac{1}{\sigma_{tot}} \frac{d\sigma(e,e'h)}{dz} = \frac{\sum_{q,\bar{q}} e_q^2 f_1^q(x) D_q^h(z)}{\sum_{q,\bar{q}} e_q^2 f_1^q(x)}. \tag{16}$$

For the quark to pion fragmentation functions $D_\pi^+(z)$ and $D_\pi^-(z)$, we follow the parameterization [25] of KKP to obtain the sum of $D_\pi^+(z) + D_\pi^-(z)$. For the ratio $D_\pi^-(z)/D_\pi^+(z)$, we use a fit to the HERMES data: $D_\pi^-/D_\pi^+ = (1-z)^{0.084}/(1+z)^{1.984}$. Kaon fragmentation functions in the KKP parameterization are used to estimate the kaon rates.

Existing data indicate that the fragmented products follow a Gaussian-like distribution in transverse momentum. For the $N(e,e'\pi)X$ reaction, recent HERMES preliminary datashowed that the transverse momentum ($P_\perp$) distribution for both π^+ and π^- follow the form of $e^{(-aP_\perp^2)}$ with $a = 3.76$ (GeV/c)$^{-2}$, corresponding to an average quark transverse momentum of $\langle P_\perp^2 \rangle = 0.26$ (GeV/c)^2. Charged kaon transverse momentum distributions are also found to be similarWe used this distribution and realistic spectrometer acceptances in a Monte Carlo simulation to estimate the count rates. The issue of hadron decay is also considered in the rate estimation. The typical survival factors for π^+ of 2.30 GeV/c momentum is 0.82, after a flight-path of 26.0 meter through HMS.

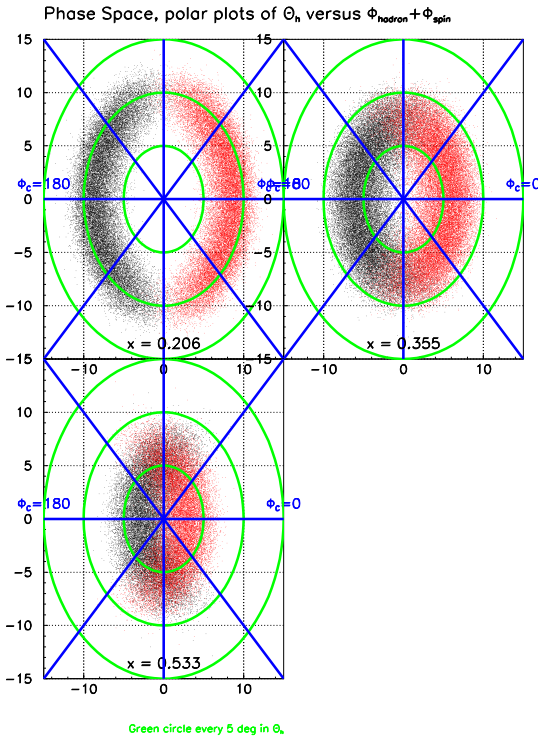

Figure 15: Angular coverage of the Collins angle $\phi_h + \phi_S^l$ are shown for each x-bin, viewed along beam. Black: $\phi_S^l = 0°$. red: $\phi_S^l = 180°$. For each x-bin the full 2π range is covered.

5.2 Statistical uncertainties of asymmetry $\mathcal{A}_{LT}$

The event rates from the NH_3 target (R^{π^+}), total number of $(e, e'\pi^+)$ events in each x-bin, the statistical uncertainties of the $\mathcal{A}_{LT}$ asymmetries corresponding to 500 hours of beam on target are listed in Table–3. We have assumed a beam current of 80 nA, beam polarization of 80%, target thickness of 3 cm, a polarization of 80% for the NH_3 target.

$\langle x \rangle$	$\langle z_\pi \rangle$	R^{π^+} Hz	N^{π^+} k	$f^{\pi^+} P_B P_T$	$\delta\mathcal{A}_{\mathcal{L}\mathcal{T}}^{\pi^+}$ %
0.206	0.44	0.12	215.4	0.141	1.53
0.355	0.48	0.06	115.3	0.153	1.92
0.533	0.52	0.02	37.4	0.164	3.16

Table 3: Coincidence event rates (R^{π^+}), the total number of events on NH_3 (N^{π^+}), the product of beam polarization, target polarization and the dilution factor ($f^{\pi^+} P_B P_T$), the expected statistical uncertainties of this experiment ($\delta\mathcal{A}_{LT}^{\pi^+}$). Data of all x-bins will be collected simultaneously.

5.3 Systematic uncertainties

With the good quality beam suitable for parity experiments which measure beam-helicity asymmetries to sub-ppm level, the 30 Hz fast beam helicity flip practically eliminates all significant systematic uncertainties associated with $\mathcal{A}_{LT}$ measurement. This is one of the most important advantages Jefferson Lab has over other lepton facilities in the world. For example, at the HERMES experiment in DESY, the positron beam helicity has only been flipped at a rate of once every few months. At the COMPASS experiment in CERN, the muon beam helicity is fixed for a given beam energy.

We plan to evenly split the 500 hour production time between the settings of target spin pointing to and away from the BigCal side. A consistency check of $\mathcal{A}_{LT}(\phi_S = 0^\circ) = -\mathcal{A}_{LT}(\phi_S = 180^\circ)$ will expose most of the remaining systematic uncertainties and false asymmetries. In the following, we list the still remaining systematic uncertainties which are common to polarized target experiments.

Relative systematic uncertainties of $\mathcal{A}_{LT}$

Knowledge of target polarization and dilution factor dominates the systematic uncertainty of $\mathcal{A}_{LT}$. The effects of radiative corrections will be treated in a Monte Carlo simulation following the procedures of the HERMES analysis, which found that the systematic uncertainties introduced by this procedure are negligible, at least in the case of A_{LL}. Kinematic smearing will also be treated following the procedure of the HERMES analysis.

Major systematic uncertainties in double-spin asymmetries $\mathcal{A}_{LT}$:	
Uncertainty in target polarization $\delta P_T/P_T$:	$\pm 2.5\%$ relative
Uncertainty in beam polarization $\delta P_B/P_B$:	$\pm 2.0\%$ relative
Helicity correlated beam charge uncertainty $\delta(Q_+/Q_-)$:	$\ll 10^{-4}$ absolute
Radiative correction and smearing:	$\pm 1.5\%$ relative
Dilution factor $\delta f^{\pi^+}/f^{\pi^+}$:	$\pm 2.5\%$ relative
Total relative systematic uncertainty of $\mathcal{A}_{LT}^{\pi^+}$	$\pm 4.3\%$

Absolute systematic uncertainties of $\mathcal{A}_{LT}$: subtracting non-zero $\mathcal{A}_{LL}$

The transverse target spin orientation is within the lab floor-plane 80° to beam-left (or 100° to beam right), the angle between the direction of the target spin and the momentum transfer $\vec{q}$ is $\theta_{qS} = 85^\circ \sim 92^\circ$ (or $\theta_{qS} = 95^\circ \sim 88^\circ$). Therefore, the longitudinal target polarization components is $|S_L|/S = |\cos\theta_{qS}| \approx 0.035 \sim 0.087$. The longitudinal target double-spin asymmetries $\mathcal{A}_{LL}$ has been measured at the HERMES kinematics and will be measured with better precision in the Hall C semi-SANE experiment at a similar kinematics. Even if we assign a much larger relative

uncertainties of $\mathcal{A}_{LL}$ to $\pm 10\%$, its contribution to the systematic uncertainties of $\mathcal{A}_{LT}$ will still be rather small at the level of $0.001 \sim 0.003$, as listed in Table 4.

$\langle x \rangle$	$\langle \theta_{qS} \rangle$	$\mathcal{A}_{LL}$	$\delta\mathcal{A}_{LT} = \lvert \cos\theta_{qS} \rvert \cdot \delta\mathcal{A}_{LL}$
0.206	84.5°	0.33	0.003
0.355	88.2°	0.43	0.001
0.533	91.9°	0.46	0.001

Table 4: The absolute systematic uncertainties of $\mathcal{A}_{LT}$ caused by non-zero longitudinal target spin component, thus the uncertainties from $\mathcal{A}_{LL}$. A relative uncertainties of $\delta\mathcal{A}_{LL}/\mathcal{A}_{LL} = \pm 10\%$ has been assigned.

Systematic uncertainties of $g_{1T}^{u(1)}/f_1^u$: neglecting d-quark contribution

As shown in Fig. 7, d-quark contributes to less than 5% of total SIDIS $p(e, e'h^+)$ cross section. Assuming g_{1T}^d follows the prediction of Kotzinian *et al.* with a sign opposite to that of g_{1T}^u, neglecting d-quark contribution will result in an overestimation of $g_{1T}^{u(1)}/f_1^u$ by a relative uncertainties of 1.6%, much less than the statistical uncertainties of this experiment.

Systematic uncertainties of $g_{1T}^{u(1)}/f_1^u$: gluon contributions and higher twist effects

Gluons can contribute to the SIDIS cross sections in general, however, these type of contribution will be higher-twist or power suppressed since gluon doesn't couple to photon directly. Moreover, since the target is a transversely polarized spin-$\frac{1}{2}$ particle and gluons carry one unit of spin, there is no known gluon distribution associated with the transverse target spin.

6 Expected Results and Impacts

With 500 hours of beam on target, we expect to have a rather good measurement on asymmetry $\mathcal{A}_{LT}$ in three x-bins. Fig. 16 shows the expected statistical uncertainties of $\mathcal{A}_{LT}$ compared with the predictions of Kotzinian *et al.*[9]. Clearly, this experiment has the capability to claim the first definitive measurement of a non-zero $\mathcal{A}_{LT}$.

Assuming u-quark dominance, the measured asymmetry $\mathcal{A}_{LT}$ can be directly translated into ratio of $g_{1T}^{u(1)}/f_1^u$. The expected statistical accuracies are shown in Fig 18 in comparison with the prediction of Kotzinian *et al.*[9] and in Fig 18 with the prediction of F. Yuan[8]. Another calculation of the revised version of Gamberg *et al.*[16] will be available in January 2007.

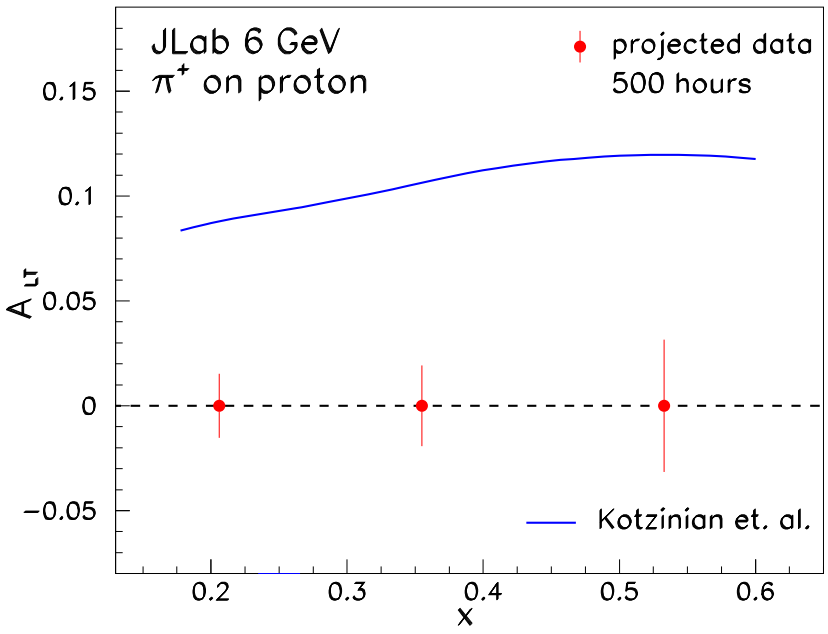

Figure 16: The projected statistical uncertainties of $\mathcal{A}_{LT}$ from this experiment are compared with the prediction of Kotzinian *et al.*

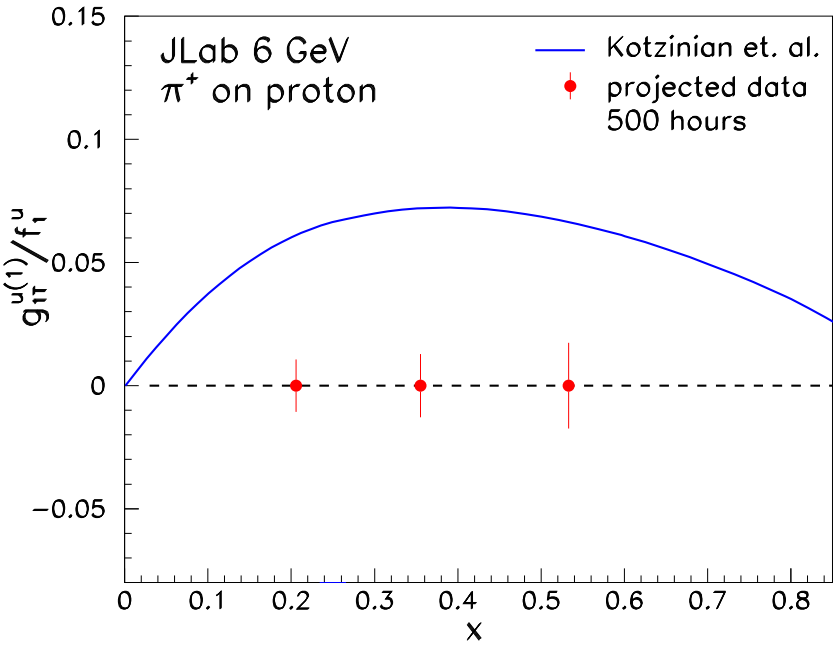

Figure 17: The projected statistical uncertainties of $g_{1T}^{u(1)}(x)/f_1^u(x)$ from this experiment are compared with the prediction of Kotzinian *et al.*

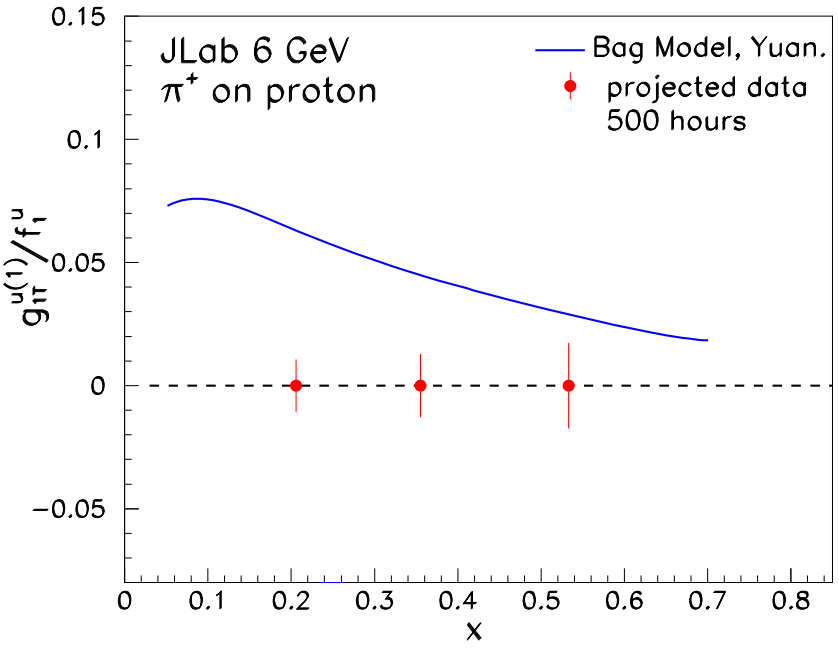

Figure 18: The projected statistical uncertainties of $g_{1T}^{u(1)}(x)/f_1^u(x)$ from this experiment are compared with the Bag Model calculation of F. Yuan.

7 Beam time request and installation time

The beam time request are listed in detail in Table 5. We request 600 hours (25 days) of beam time in total, of which 500 hours is for beam on the polarized target. A large amount of overhead time (100 hours total) is requested mostly for target related activities. This overhead time can be shared with other experimental activities, such as Möller measurements and unpolarized target measurements, as has been done in the past during other Hall C polarized target experiments. Target anneals can also be arranged to coincide with the scheduled accelerator maintenance activities in order to save overhead time. The target spin direction will be flipped every time target is annealed, without causing extra down time than necessary.

Beam on polarized NH_3 target	**500** hour
Target overhead, Möller runs and ^{12}C target runs.	**100** hour
Total Time Request	**600 (25 days)**

Table 5: Details of the beam time request.

Since the set-up of this experiment is exactly identical to that of the transverse target running of the SANE experiment, a considerable fraction of this experiment (200 hours plus overhead) can run concurrently with the SANE experiment. See Appendix-I for the original table of beam time request of the SANE experiment. **Under such a condition, the total beam request of this experiment is 15 days.**

Although this experiment requires a large effort in installation, we point out here that the same installation effort will allow consequent running of four experiments, namely the SANE and semi-SANE experiments and the wide-angle Compton experiment.

8 By-products of this experiment

With extra 300 hours beam time added to the transverse SANE run, better precisions in inclusive asymmetries and structure function g_2^p, thus the d_2^p moment, can be reached. The statistical uncertainties will be reduced to 63% of that of SANE.

With many target spin flips and summing over beam helicity, this experiment will also yield data for target singles spin A_{UT}. The Collins moment of A_{UT}, which depends on $\sin(\phi_h + \phi_S)$, will be extracted with some reasonable precisions since this experiment covers the full 2π range of the Collins angle as shown in Fig. 15 Our coverage on the Sivers angle, $\phi_h - \phi_S$ is not as good as shown in Fig.14.

A much detailed impact study of this experiment on Collins and Sivers asymmetry measurement will be presented at PAC31.

9 Relation with other experiments

- HERMES experiment collected data in 2002-2004 on a transversely polarized proton target. Since the main goal of HERMES is to obtain target single-spin asymmetry A_{UT}, part of data were collected with low positron beam polarization. The beam helicity at HERMES can only be flipped once every few months, make it rather challenging to extract beam helicity asymmetries. While the HERMES spectrometer has a good $\sin\phi$ coverage, it has an unfavorable $\cos\phi_h - \phi_S$ coverage due to its geometrical features. Furthermore, compare with this experiment the HERMES event sample are dominately at a lower x region where asymmetry $\mathcal{A}_{LT}$ is expected to be smaller.

- COMPASS experiment collected data in 2002 and 2004 on a transversely polarized ^{6}LiD target to obtain single-spin asymmetry A_{UT}. Since the muon beam at COMPASS has fixed helicity corresponding to a fixed beam energy, it is rather challenging to extract double-spin asymmetry $\mathcal{A}_{LT}$. In addition, $\mathcal{A}_{LT}$ on a deuteron is expected to be smaller than that of a proton, and at the COMPASS kinematics ($x < 0.1$), $\mathcal{A}_{LT}$ is expected to be even smaller than the valence region.

  Hall B polarized target data were originally collected for inclusive measurements in order to extract A_{1p} and A_{1d}. Part of data taken in year 2000 with 5.7 GeV beam (EG1b) can be analyzed for $(e, e'\pi)$ reactions. However, the physics goals addressed in this proposal can not be achieved in analyzing the existing EG1b data. The much higher luminosity, the much better coverage in deep inelastic kinematics, and the precision knowledge on acceptance, particle identification and detector efficiency make this proposal unique at Jefferson Lab.

- The CLAS detector in JLab Hall B does not have the capability to run with a transversely polarized target.

- JLab 12 GeV upgrade. Transverse spin physics through semi-inclusive DIS is promised to be a major highlight of Jefferson Lab's 12 GeV physics program. With the exploratory first investigation of this experiment to open up new directions in SIDIS physics, much needed guidances and motivations can be provided through this experiment to Jefferson Lab's 12 GeV transverse spin program.

10 Manpower and collaboration

The core group of people currently in the collaboration can provide enough manpower to run this experiment. In addition, we expect other groups, such as those involved in the Hall A neutron transversity experiments, Hall C SANE and semi-SANE experiments, the HERMES and COMPASS experiment, to join the collabo-

ration and to bring their expertise and knowledge to this experiment and to extend their roles into the physics program of Jefferson Lab's 12 GeV upgrade.

The Yerevan group will continue its traditional role in supporting hardware works in Hall C experiments. In particular for this experiment, the Yerevan group will take the responsibility of the BigCal calorimeter hardware work should needs be identified beyond that of SANE and semi-SANE.

The Rutgers group will take the responsibility of the BigCal trigger electronics, extending its role in Gep-III, Gep-2γ experiments as well as in SANE and semi-SANE experiments. The coincidence trigger electronics between the BigCal calorimeter and HMS should have been already set up during the Gep-III and Gep-2γ experiments which are scheduled to start running in the summer of 2007. The Rutgers group will take the responsibility of further hardware check and debugging of the coincidence trigger for this experiment, as well as for the semi-SANE experiment. In addition, the Rutgers group will take the responsibility of physics simulation and part of the physics data analysis work.

The JLab Hall C group will take the responsibility for the operation of the HMS spectrometer in its standard configuration. In addition, the Hall C group will take the responsibility of the data acquisition system, slow control and on-line detector monitoring software.

11 Summary

This experiment will be the first time that a transversely polarized proton target being used in a semi-inclusive DIS measurement at Jefferson Lab. The goal of this experiment is to make the first definitive measurement of the double-spin asymmetry $\mathcal{A}_{LT}$ and the quark transverse momentum dependent distribution g_{1T} and to clearly establish if it is non-zero. This experiment can also be viewed as an exploratory effort to open up un-chattered territory in SIDIS physics and to provide much needed guidances and motivations for the transverse target SIDIS program with Jefferson Lab's 12 GeV upgrade.

The technical details of this experiment is mostly identical to that of the approved "semi-SANE" (E04-113) and "SANE" (E03-109) experiments. No extra hardware preparation work is needed beyond the setting up of the coincidence trigger between *BETA* and HMS, which is also part of the semi-SANE preparation. The collaboration has proper manpower and expertise to cover the shifts of the running time and the target overhead beyond the needs of SANE and semi-SANE. A total of 25 days of 6 GeV beam are needed for this experiment of which 10 days can be a shared time with the SANE experiment. **Therefore, we request approval of 15 days assuming the SANE experiment is re-approved.**

12 Acknowledgment

We thank D. Boer, P. Mulders, A Metz and M. Anselmino for many discussions. We thank F. Yuan, L. Gamberg, B. Parsamyan and A. Kotzinian for providing their calculations.

A Appendix-I: the original SANE experiment beam time request

The original SANE experiment beam time request[23]. The 200 hour transverse target running listed under 6.0 GeV and $\theta_N = 80^\circ$ and its associated overhead time can be shared with this proposal. The total beam time which can be shared amounted to 10 PAC days.

E_{beam} (GeV)	I (nA)	θ_N (°)	θ_e (°)	Time (h)
6.0	85	180	40	100
6.0	85	80	40	200
4.8	85	180	40	70
4.8	85	80	40	130
2.4	1000	26	58	10
Packing Fraction				20
Moller Measurements				21
Beam Time				551
Target anneals				62
Energy change				48
Target Rotation				48
Stick Changes				48
Overhead Time				206
SANE Requested Time				654

References

1. A. Airapetian *et al.*, Phys. Rev. Lett. **94**, 012002 (2005).
2. V. Y. Alexakhin *et al.*, Phys. Rev. Lett. **94**, 202002 (2005).
3. P. Mulders and R. D. Tangerman *Nucl. Phys.* B **461**, 197 (1996)
4. X. D. Ji, J. P. Ma and F. Yuan, Phys. Rev. D **71**, 034005 (2005). Phys. Lett. B **597**, 299 (2004).
5. J. C. Collins and A. Metz, Phys. Rev. Lett. **93**, 252001 (2004).
6. D. Boer and P. Mulders, *Phys. Rev.* D **57**, 5780 (1998)
7. R. Jacob, P. J. Mulders and J. Rodrigues, Nucl. Phys. **A626**, 937 (1997).
8. F. Yuan, Phys. Lett. **B575**, 45 (2003), and private communications (2006).
9. A. Kotzinian, B. Parsamyan and A. Prokudin, *Phys. Rev.* D **73**, 114017 (2006).
10. J. C. Collins, Phys. Lett. B **536** (2002) 43.
11. R. Kundu and A. Metz, Phys. Rev. D **65** (2002) 014009.
12. M. Schlegel and A. Metz, arXiv:hep-ph/0406289.
13. K. Goeke, A. Metz, P. V. Pobylitsa and M. V. Polyakov, Phys. Lett. B **567** (2003) 27.
14. Alessandro Bacchetta, Umberto D'Alesio, Markus Diehl, C. Andy Miller, *Phys. Rev.* D **70**, 117504 (2004).
15. A. Bacchetta, hep-ph/0307282.
16. L.P. Gamberg, D.S. Hwang and K.A.Oganessyan *Phys. Lett.* B **584**, 276 (2004), and private communications (2006).
17. S. Wandzura and F. Wilczek, Phys. Lett. **B72**, 195 (1977).
18. A. Kotzinian and P.J. Mulders, Phys. Rev. **D54**, 1229 (1996).
19. M. Gluck, E. Reya and A. Vogt, Eur. Phys. J. C **5**, 461 (1998).
20. M. Gluck, E. Reya, M. Stratmann and W. Vogelsang, Phys. Rev. D **63**, 094005 (2001).
21. S. Kretzer, Phys. Rev. D **62**, 054001 (2000).
22. JLab-PAC26 proposal E04-113, "Semi-Inclusive Spin Asymmetries on the Nucleon Experiment" (semi-SANE), X. Jiang, P. Bosted, D. Day and M. Jones co-spokespersons.
23. JLab-PAC24 proposal E03-109, "Spin Asymmetries on the Nucleon Experiment" (SANE), S. Choi, Z.-E. Meziani and O.A. Rondon co-spokespersons.
24. Lai, H.L. *et al.*, *Eur. Phys. J.* **C12**, 375 (2000).
25. B. A. Kniehl, G. Kramer, and B. Potter, *Nucl. Phys.* B **582**, 514 (2000).